



## Self-Motions of 3-RPS Manipulators

Josef Schadlbauer, Manfred Husty, Stéphane Caro, Philippe Wenger

### ► To cite this version:

Josef Schadlbauer, Manfred Husty, Stéphane Caro, Philippe Wenger. Self-Motions of 3-RPS Manipulators. *Frontiers of Mechanical Engineering*, 2013, 8 (1), pp.62-69. 10.1007/s11465-013-0366-3 . hal-00914024

**HAL Id: hal-00914024**

**<https://hal.science/hal-00914024>**

Submitted on 19 Nov 2014

**HAL** is a multi-disciplinary open access archive for the deposit and dissemination of scientific research documents, whether they are published or not. The documents may come from teaching and research institutions in France or abroad, or from public or private research centers.

L'archive ouverte pluridisciplinaire **HAL**, est destinée au dépôt et à la diffusion de documents scientifiques de niveau recherche, publiés ou non, émanant des établissements d'enseignement et de recherche français ou étrangers, des laboratoires publics ou privés.

# Self-Motions of 3-RPS Manipulators

Josef Schadlbauer\*, Manfred L. Husty\*,  
Stéphane Caro<sup>†</sup>, Philippe Wenger<sup>†</sup>

**Abstract:** Recently a complete kinematic description of the 3-RPS parallel manipulator was obtained using algebraic constraint equations. It turned out that the workspace splits into two components describing two kinematically different operation modes. In this paper the algebraic description is used to give a complete analysis of all possible self-motions of this manipulator in both operation modes. Furthermore it is shown that a transition from one operation mode into the other in a self-motion is possible.

**Keywords:** 3-RPS-manipulator, singularity, self motion.

## 1 Introduction

A 3-RPS manipulator is a three degree of freedom (3-DOF) parallel manipulator. It consists of an equilateral triangular fixed platform and a similar moving platform connected by three identical RPS legs. The first joint (R-joint) is connected to the base and the last joint (S-joint) is connected to the moving platform (see Fig. 1). The legs are extensible, changing lengths via prismatic joints (P-joints), thereby moving the platform with three highly coupled DOFs. In the past few years the 3-RPS obtained a lot of attention in the kinematics community, see e.g. [?]. In [?] an overview of existing results can be found and especially it is stated that Hunt [?] introduced this type of lower-mobility parallel manipulator. In [?] Gallardo et al. present a kinematic analysis of the manipulator including position, velocity and acceleration behavior using vector loop equations for the position analysis and screw theory for velocity and acceleration analysis. Bonev [?] lists the manipulator among the zero torsion parallel manipulators. Huang et al. [?] present an analysis of the instantaneous motion capability of the manipulator using screw theory. They discuss the distribution of twist axes only in three different configurations of the manipulator: (a) platform and base are parallel at the considered instant, (b) the platform rotates about an axis coincident with one side of the platform triangle and (c) a “general mode”. Because of the local nature of this method several particularities of the global behaviour of this mechanism were overlooked. Already Tsai [?] reports the correct number of solutions of the direct kinematics, but as it turned out, due to the applied local methods (also in [?]), a complete description of operation modes and singular poses was overlooked. This gap was partially closed by Basu and Ghosal [?], who gave a characterization of special singular poses of the manipulator.

In [?], using an algebraic description of the manipulator, together with *Study*’s kinematic mapping, a complete characterization of the forward kinematics, the operation modes, the singular poses and the transitions between the operation modes was given. It turned out that the manipulator has two kinematically different operation modes. **The first one is characterized by finite  $\pi$ -screws. Axes of these screws are tilted with respect to the base and the translation distance depends on the chosen axis. The**

---

\*Institute for Basic Sciences in Engineering, Unit for Geometry and CAD, University of Innsbruck, Austria, e-mail: {josef.schadlbauer, manfred.husty}@uibk.ac.at

<sup>†</sup>Institut de Recherche en Communications et Cybernétique de Nantes, France, e-mail: {stephane.caro, philippe.wenger}@ircyn.ec-nantes.fr

second mode has horizontal screw axes with rotation angle and translation distance depending on the chosen axis. Note, that this characterization refers to finite screws and not instantaneous screws. The singularities in both operations modes were derived in kinematic image space as well as in the joint space. In joint space the singularity surfaces are of degree 24 and it was shown that for input joint combinations fulfilling an eight order polynomial transition from one operation mode to the other is possible.

In this paper the self motions of this manipulator will be discussed. The paper is organized as follows: In Section 2 a description of the architecture of the 3-RPS is given and the set of constraint equations is recalled. In Section 3 the possible self-motions for each operation mode are derived. Section 4 presents a method to transform the self-motions into a standard form and in Section 5 it is shown that a transition from one operation mode into the other via a self-motion is possible.

It should be noted that the 3-RPS manipulator is a special case of the 6 – 3 Stewart-Gough platform. The self-motion of this type of manipulator was discussed in Karger [?]. As opposed to Krager’s study we can prove that the classification of the self-motions of the 3-RPS manipulator presented in this paper is complete.

## 2 Robot Design

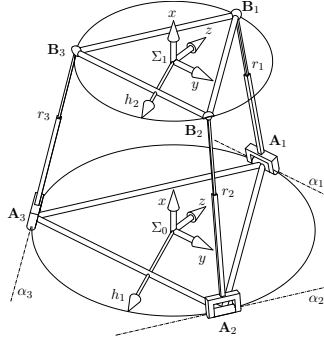


Figure 1: Design of the 3-RPS parallel robot

With respect to Fig. 1 we consider the 3-RPS parallel manipulator with the following architecture: The base of the 3-RPS consists of an equilateral triangle with vertices  $\mathbf{A}_1$ ,  $\mathbf{A}_2$  and  $\mathbf{A}_3$  and circumradius  $h_1$ . The origin of the fixed frame  $\Sigma_0$  coincides with the circumcenter of the triangle  $\mathbf{A}_1$ ,  $\mathbf{A}_2$  and  $\mathbf{A}_3$ . The  $yz$ -plane of  $\Sigma_0$  is defined by the plane  $\mathbf{A}_1$ ,  $\mathbf{A}_2$ ,  $\mathbf{A}_3$ . Finally,  $\mathbf{A}_1$  lies on the  $z$ -axis of  $\Sigma_0$ . In the platform there is another equilateral triangle with vertices  $\mathbf{B}_1$ ,  $\mathbf{B}_2$  and  $\mathbf{B}_3$  and circumradius  $h_2$ . The circumcenter of the triangle  $\mathbf{B}_1$ ,  $\mathbf{B}_2$  and  $\mathbf{B}_3$  lies in the origin of  $\Sigma_1$ , which is the moving frame. Again, the plane defined by  $\mathbf{B}_1$ ,  $\mathbf{B}_2$  and  $\mathbf{B}_3$  coincides with the  $yz$ -plane of  $\Sigma_1$  and  $\mathbf{B}_1$  lies on the  $z$ -axis of  $\Sigma_1$ . The two design parameters  $h_1$  and  $h_2$  are taken to be strictly positive numbers. Now each pair of vertices  $\mathbf{A}_i$ ,  $\mathbf{B}_i$  ( $i = 1, \dots, 3$ ) is connected by a limb, with a rotational joint at  $\mathbf{A}_i$  and a spherical joint at  $\mathbf{B}_i$ . The length of each limb is denoted by  $r_i$  and is adjusted via an actuated prismatic joint. The axes  $\alpha_i$  of the rotational joints at  $\mathbf{A}_i$  are tangent to the circumcircle and therefore lie within the  $yz$ -plane of  $\Sigma_0$ . Overall we have five parameters, namely  $h_1$ ,  $h_2$ ,  $r_1$ ,  $r_2$  and  $r_3$ . While  $h_1$  and  $h_2$  determine the design of the manipulator, the parameters  $r_1$ ,  $r_2$  and  $r_3$  are joint parameters, which determine the motion of the robot. We can consider the joint parameters to be like design parameters when they are assigned with specific leg lengths  $r_i$ . In some computations the leg lengths  $r_i$  will be replaced with their squares which then will be denoted by  $R_i$ . Deriving the constraint equations is one essential step in solving the kinematics of a manipulator. To compute these equations, which describe the motion capability, the direct kinematics and also the singularities of the manipulator, we use the *Study*-parameterization of the motion group  $SE(3)$ . The vertices of the base triangle and the platform triangle in  $\Sigma_0$  resp.  $\Sigma_1$  are

$$\begin{aligned}\mathbf{A}_1 &= (1 : 0 : 0 : h_1), & \mathbf{A}_2 &= (1 : 0 : \sqrt{3}h_1/2 : -h_1/2), & \mathbf{A}_3 &= (1 : 0 : -\sqrt{3}h_1/2 : -h_1/2) \\ \mathbf{b}_1 &= (1 : 0 : 0 : h_2), & \mathbf{b}_2 &= (1 : 0 : \sqrt{3}h_2/2 : -h_2/2), & \mathbf{b}_3 &= (1 : 0 : -\sqrt{3}h_2/2 : -h_2/2)\end{aligned}$$

thereby using projective coordinates with the homogenizing coordinate as first **entry**. To avoid confusion, coordinates with respect to  $\Sigma_0$  are written in capital letters and those with respect to  $\Sigma_1$  are in lower case. To obtain the coordinates  $\mathbf{B}_1$ ,  $\mathbf{B}_2$  and  $\mathbf{B}_3$  of  $\mathbf{b}_1$ ,  $\mathbf{b}_2$  and  $\mathbf{b}_3$  with respect to  $\Sigma_0$  a coordinate transformation has to be applied. To describe this coordinate transformation we use *Study's* parameterization of a spatial Euclidean transformation matrix  $\mathbf{M} \in SE(3)$  (for detailed information on this approach see [?, ?, ?]).

$$\begin{aligned}\mathbf{M} &= \begin{pmatrix} x_0^2 + x_1^2 + x_2^2 + x_3^2 & \mathbf{0}^\top \\ \mathbf{M}_T & \mathbf{M}_R \end{pmatrix}, & \mathbf{M}_T &= \begin{pmatrix} 2(-x_0y_1 + x_1y_0 - x_2y_3 + x_3y_2) \\ 2(-x_0y_2 + x_1y_3 + x_2y_0 - x_3y_1) \\ 2(-x_0y_3 - x_1y_2 + x_2y_1 + x_3y_0) \end{pmatrix} \\ \mathbf{M}_R &= \begin{pmatrix} x_0^2 + x_1^2 - x_2^2 - x_3^2 & 2(x_1x_2 - x_0x_3) & 2(x_1x_3 + x_0x_2) \\ 2(x_1x_2 + x_0x_3) & x_0^2 - x_1^2 + x_2^2 - x_3^2 & 2(x_2x_3 - x_0x_1) \\ 2(x_1x_3 - x_0x_2) & 2(x_2x_3 + x_0x_1) & x_0^2 - x_1^2 - x_2^2 + x_3^2 \end{pmatrix}\end{aligned}$$

The vector  $\mathbf{M}_T$  represents the translational part and  $\mathbf{M}_R$  represents the rotational part of the transformation  $\mathbf{M}$ . The parameters  $x_0, x_1, x_2, x_3, y_0, y_1, y_2, y_3$  which appear in the matrix  $\mathbf{M}$  are called *Study-parameters* of the transformation  $\mathbf{M}$ . The mapping

$$\kappa: SE(3) \rightarrow P \in \mathbb{P}^7 \quad (1)$$

$$\mathbf{M}(x_i, y_i) \mapsto (x_0 : x_1 : x_2 : x_3 : y_0 : y_1 : y_2 : y_3)^T \neq (0 : 0 : 0 : 0 : 0 : 0 : 0 : 0)^T$$

is called *kinematic mapping* and maps each Euclidean displacement of  $SE(3)$  to a point  $P$  on a quadric  $S_6^2 \subset \mathbb{P}^7$ . In this way, every projective point  $(x_0 : x_1 : x_2 : x_3 : y_0 : y_1 : y_2 : y_3) \in \mathbb{P}^7$  represents a spatial Euclidean transformation, if it fulfills the following equation  $S_6^2: x_0y_0 + x_1y_1 + x_2y_2 + x_3y_3 = 0$  and inequality:  $x_0^2 + x_1^2 + x_2^2 + x_3^2 \neq 0$  (see [?]).

The coordinates of  $\mathbf{b}_i$  with respect to  $\Sigma_0$  are obtained by:

$$\mathbf{B}_i = \mathbf{M} \cdot \mathbf{b}_i, \quad i = 1, \dots, 3.$$

Now, as the coordinates of all vertices are given in terms of the transformation parameters  $x_0, x_1, x_2, x_3, y_0, y_1, y_2, y_3$  and the design constants, we obtain constraint equations by examining the geometry of the manipulator more closely. First of all the limb connecting  $\mathbf{A}_i$  and  $\mathbf{B}_i$  has to be orthogonal to the corresponding rotational axis  $\alpha_i$ . That means, the scalar product of the vector connecting  $\mathbf{A}_i\mathbf{B}_i$  and the direction of  $\alpha_i$  vanishes. After computing this product and removing the common denominator  $(x_0^2 + x_1^2 + x_2^2 + x_3^2)$  the following equations are obtained:

$$\begin{aligned}\tilde{g}_1 &: x_0y_2 - x_1y_3 - x_2y_0 + x_3y_1 - h_2x_2x_3 + h_2x_0x_1 = 0 \\ \tilde{g}_2 &: 4\sqrt{3}h_2x_0x_1 + 2\sqrt{3}h_2x_2x_3 - 2\sqrt{3}x_0y_2 + 2\sqrt{3}x_1y_3 + 2\sqrt{3}x_2y_0 - 2\sqrt{3}x_3y_1 \\ &\quad + 3h_2x_2^2 - 3h_2x_3^2 - 6x_0y_3 - 6x_1y_2 + 6x_2y_1 + 6x_3y_0 = 0 \\ \tilde{g}_3 &: 4\sqrt{3}h_2x_0x_1 + 2\sqrt{3}h_2x_2x_3 - 2\sqrt{3}x_0y_2 + 2\sqrt{3}x_1y_3 + 2\sqrt{3}x_2y_0 - 2\sqrt{3}x_3y_1 \\ &\quad - 3h_2x_2^2 + 3h_2x_3^2 + 6x_0y_3 + 6x_1y_2 - 6x_2y_1 - 6x_3y_0 = 0,\end{aligned}$$

which after some elementary manipulations ( $g_1 = \frac{1}{3h_2}[\frac{1}{4\sqrt{3}}(\tilde{g}_2 + \tilde{g}_3) + \tilde{g}_1]$ ,  $g_2 = \frac{1}{6}(\tilde{g}_2 - \tilde{g}_3)$ ,  $g_3 = \frac{1}{4\sqrt{3}}(\tilde{g}_2 + \tilde{g}_3)$ ) simplify to:

$$\begin{aligned}g_1 &: x_0x_1 = 0 \\ g_2 &: h_2x_2^2 - h_2x_3^2 - 2x_0y_3 - 2x_1y_2 + 2x_2y_1 + 2x_3y_0 = 0 \\ g_3 &: 2h_2x_0x_1 + h_2x_2x_3 - x_0y_2 + x_1y_3 + x_2y_0 - x_3y_1 = 0.\end{aligned} \quad (2)$$

Next we make use of the limb lengths. In the direct kinematics the joint parameters are given, therefore the distance between  $\mathbf{A}_i$  and  $\mathbf{B}_i$  has to be  $r_i = \text{const}$  and from this follows that  $\mathbf{B}_i$  has the freedom to move along a circle with center  $\mathbf{A}_i$ , which lies in a plane perpendicular to  $\alpha_i$ . The constraint equation for this distance property has been derived in [?] for the direct kinematics of the general 6-SPS-Stewart-Gough-platform. Applying this formula for the design parameters at hand we obtain:

$$\begin{aligned}
g_4 : & (h_1 - h_2)^2 x_0^2 + (h_1 + h_2)^2 x_1^2 + (h_1 + h_2)^2 x_2^2 + (h_1 - h_2)^2 x_3^2 + 4(h_1 - h_2)x_0y_3 + 4(h_1 + h_2)x_1y_2 \\
& - 4(h_1 + h_2)x_2y_1 - 4(h_1 - h_2)x_3y_0 + 4(y_0^2 + y_1^2 + y_2^2 + y_3^2) - (x_0^2 + x_1^2 + x_2^2 + x_3^2)R_1 = 0 \\
g_5 : & (h_1 - h_2)^2 x_0^2 + (h_1 + h_2)^2 x_1^2 + (h_1^2 + h_2^2 - h_1h_2)x_2^2 + (h_1^2 + h_2^2 + h_1h_2)x_3^2 - 2(h_1 \\
& - h_2)x_0y_3 - 2(h_1 + h_2)x_1y_2 + 2(h_1 + h_2)x_2y_1 + 2(h_1 - h_2)x_3y_0 - 2\sqrt{3}(h_1 \\
& - h_2)x_0y_2 + 2\sqrt{3}(h_1 + h_2)x_1y_3 + 2\sqrt{3}(h_1 - h_2)x_2y_0 - 2\sqrt{3}(h_1 + h_2)x_3y_1 \\
& - 2\sqrt{3}h_1h_2x_2x_3 + 4(y_0^2 + y_1^2 + y_2^2 + y_3^2) - (x_0^2 + x_1^2 + x_2^2 + x_3^2)R_2 = 0 \\
g_6 : & (h_1 - h_2)^2 x_0^2 + (h_1 + h_2)^2 x_1^2 + (h_1^2 + h_2^2 - h_1h_2)x_2^2 + (h_1^2 + h_2^2 + h_1h_2)x_3^2 - 2(h_1 \\
& - h_2)x_0y_3 - 2(h_1 + h_2)x_1y_2 + 2(h_1 + h_2)x_2y_1 + 2(h_1 - h_2)x_3y_0 + 2\sqrt{3}(h_1 \\
& - h_2)x_0y_2 - 2\sqrt{3}(h_1 + h_2)x_1y_3 - 2\sqrt{3}(h_1 - h_2)x_2y_0 + 2\sqrt{3}(h_1 + h_2)x_3y_1 \\
& + 2\sqrt{3}h_1h_2x_2x_3 + 4(y_0^2 + y_1^2 + y_2^2 + y_3^2) - (x_0^2 + x_1^2 + x_2^2 + x_3^2)R_3 = 0.
\end{aligned}$$

$R_i$  in the equations for  $g_4, g_5, g_6$  denote the squares of the input parameters  $r_i$  (leg lengths). To complete the system, we add the Study-equation ( $g_7$ ), because all the solutions have to be within the Study-quadric and a normalizing condition ( $g_8$ ).

$$g_7 : x_0y_0 + x_1y_1 + x_2y_2 + x_3y_3 = 0, \quad g_8 : x_0^2 + x_1^2 + x_2^2 + x_3^2 = 1 \quad (3)$$

The set of equations describing a general 3-RPS manipulator forms the ideal

$$\mathcal{I} = \langle g_1, g_2, g_3, g_4, g_5, g_6, g_7, g_8 \rangle. \quad (4)$$

From the first equation in this set it is obvious, that this ideal consists of two components  $\mathcal{K}_1 = \langle x_0, g_2, g_3, g_4, g_5, g_6, g_7, g_8 \rangle$  and  $\mathcal{K}_2 = \langle x_1, g_2, g_3, g_4, g_5, g_6, g_7, g_8 \rangle$ . It was shown in [?] that these two components can be treated separately to compute the direct kinematics and the singularities. Therefore the same can be done for computing the self-motions of this manipulator type.

### 3 Self-motions

In the following subsections we will derive conditions on the input parameters, such that the manipulator can perform at least a one degree of freedom self motion.

#### 3.1 Case 1: $x_0 = 0$

By suitable scaling of the manipulator we can set, without loss of generality,  $h_1 = 1$ . Then one can compute an ordered Groebner basis of the ideal  $\mathcal{K}_1$  and this yields a univariate polynomial  $F_1$  of degree eight in one variable (e.g.  $x_2$ ) having only even powers

$$F_1 : a_0x_2^8 + b_0x_2^6 + c_0x_2^4 + d_0x_2^2 + f_0 = 0, \quad (5)$$

where  $a_0, b_0, c_0, d_0, f_0$  are polynomials in the input parameters  $R_1, R_2, R_3$  and the design parameter  $h_2$ . The polynomial  $f_0$ , being the absolute term in  $F_1$  is

$$\begin{aligned}
f_0 : & (R_2 - R_3)^4(R_2^2 - 6R_2h_2^2 - 2R_2R_3 - 24R_2 - 24R_2h_2 - 24R_3 + 9h_2^4 + \\
& 72h_2^3 + 144h_2 + R_3^2 + 180h_2^2 - 24h_2R_3 - 6h_2^2R_3).
\end{aligned} \quad (6)$$

To obtain a self-motion all coefficient polynomials  $a_0, b_0, c_0, d_0, f_0$  in Eq. 5 have to vanish simultaneously. Therefore one has to discuss the ideal  $\mathcal{L} = \langle a_0, b_0, c_0, d_0, f_0 \rangle$ . From Eq. (6) it is obvious, that there are two cases: either the first or the second factor in this polynomial has to vanish.

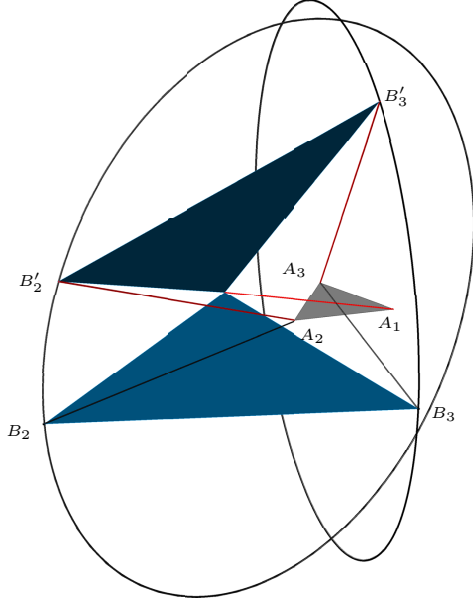


Figure 2: Two poses of the self-motion (Case 1a)

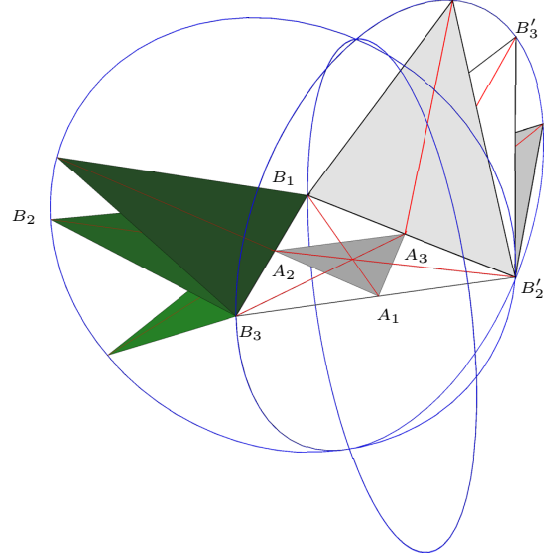


Figure 3: Special case  $h_2 = 2$

**Case 1a:**  $R_2 = R_3, h_2 \neq 0$  In this case one can compute a Groebner basis of the ideal  $\mathcal{L}$ . The Hilbert dimension of  $\mathcal{L}$  is zero, which means: there are discrete values of  $R_i$ , which allow self motion. The solutions are

$$L_1 : R_1 = 3h_2^2 + 6h_2, R_2 = R_3 = 0, \quad L_2 : R_1 = 9, R_2 = R_3 = 3h_2^2 - 3 \quad (7)$$

$L_1$  does not give any real solutions, but  $L_2$  yields for every design parameter  $h_2 > 1$  exactly one leg combination that results in a real self motion. During the motion one leg stays fixed and the moving platform performs a spherical four-bar motion. The two moving vertices of the platform run on circles contained in a sphere, centered at the fixed third vertex. Fig.2 shows an example ( $h_2 = 3, h_1 = 1$ ) of the 3-RPS manipulator in two poses of the self motion. Two motion paths of the vertices of the blue moving platform are shown. The transformation matrix reads

$$\mathbf{T}_0 = \begin{pmatrix} 1 & 0 & 0 & 0 \\ -\frac{4\sqrt{3}}{3}A_0B_0 & \frac{7}{9} - \frac{8}{3}t^2 & \frac{4}{3}A_0t & \frac{4\sqrt{3}}{9}A_0B_0 \\ -2\sqrt{3}B_0t & \frac{4}{3}A_0t & 2t^2 - 1 & \frac{2\sqrt{3}}{3}B_0t \\ \frac{1}{3} - 2t^2 & \frac{4\sqrt{3}}{9}A_0B_0 & \frac{2\sqrt{3}}{3}B_0t & \frac{2}{3}t^2 - \frac{7}{9} \end{pmatrix} \quad (8)$$

where  $A_0 = \sqrt{2 - 3t^2}$  and  $B_0 = \sqrt{\frac{1}{3} + t^2}$ ,  $t \in I \subset \mathbb{R}$ .

**Case 1b:**  $R_2 \neq R_3, h_2 \neq 0$  The second polynomial in Eq.(6) yields after computation of a Groebner basis the two symmetric cases to Case 1a ( $R_1 = R_3$  resp.  $R_1 = R_2$ ).

**Special case**  $h_2 = 2$  In this case the circumcircle of one platform triangle is the incircle of the other one. Eq.(7)( $L_2$ ) yields three identical leg lengths which have the same lengths as the heights of the bigger triangle. Therefore the manipulator (at least theoretical) can come into a folded pose, as shown in Fig.3. From this pose the manipulator can fold up in three different ways, thereby rotating about each of the base revolute axes. In the case of a 6-3 Stewart-Gough platform this motion was named butterfly motion by A. Karger in [?].

### 3.2 Case 2: $x_1 = 0$

Like in Case 1 a Groebner basis of the ideal  $\mathcal{K}_2$  can be computed and this yields a univariate polynomial  $F_2$  in  $x_3$ .

$$a_1 x_3^8 + b_1 x_3^6 + c_1 x_3^4 + d_1 x_3^2 + f_1 = 0, \quad (9)$$

where  $a_1, b_1, c_1, d_1, f_1$  are polynomials in the input parameters  $R_1, R_2, R_3$  and the design parameter  $h_2$ . The condition for the existence of a self motion is that all coefficients of Eq.(9) must vanish. The absolute term in this equation, the polynomial  $f_1$  reads

$$f_1 : -(R_2 - R_3)^4 (R_2^2 - 24R_2 - 6R_2 h_2^2 - 2R_2 R_3 + 24R_2 h_2 - 144h_2 - 24R_3 - 6h_2^2 R_3 + 180h_2^2 + 24h_2 R_3 - 72h_2^3 + R_3^2 + 9h_2^4). \quad (10)$$

Again, one has to discuss the ideal formed by the coefficient polynomials  $\mathcal{M} = \langle a_1, b_1, c_1, d_1, f_1 \rangle$  of Eq.(9). Two subcases are to be distinguished.

**Case 2a:**  $R_2 = R_3$  Substituting  $R_2 = R_3$  into the ideal  $\mathcal{M}$  yields

$$\begin{aligned} \mathcal{M}_0 = & \langle 24h_2^2(h_2 - 2)^2(-3R_1 + 6h_2 R_1 - 18h_2 - R_1 R_3 + 3R_3 + 12h_2 R_3 + R_3^2 - 6h_2^2 R_3 + 9h_2^4 - \\ & 3h_2^2 R_1 + 45h_2^2 - 36h_2^3)^2, h_2^4(R_3^2 - 24R_1 + 9h_2^4 - 72h_2^3 + 180h_2^2 - 6h_2^2 R_1 - 6h_2^2 R_3 + \\ & 24h_2 R_1 + 24h_2 R_3 - 24R_3 - 144h_2 - 2R_1 R_3 + R_1^2)^2, -2h_2^3(h_2 - 2)(-3R_1 + 6h_2 R_1 - 18h_2 - \\ & R_1 R_3 + 3R_3 + 12h_2 R_3 + R_3^2 - 6h_2^2 R_3 + 9h_2^4 - 3h_2^2 R_1 + 45h_2^2 - 36h_2^3)(R_3^2 - 24R_1 + \\ & 9h_2^4 - 72h_2^3 + 180h_2^2 - 6h_2^2 R_1 - 6h_2^2 R_3 + 24h_2 R_1 + 24h_2 R_3 - 24R_3 - 144h_2 - 2R_1 R_3 + R_1^2) \rangle \end{aligned} \quad (11)$$

Closer inspection of  $\mathcal{M}_0$  shows that it consists of three different polynomials from which  $R_i$  should be determined. But the term  $(h_2 - 2)$  is a factor of two of the three polynomials. Therefore, when  $h_2 = 2$  (the moving platform is twice as big as the fixed one), then only one polynomial remains and this reduces after substitution to  $R_1 = R_3$ . This means, in the case  $x_1 = 0$  there is the line  $R_1 = R_2 = R_3$  in the joint parameter space, which yields a self motion. Or, whenever this manipulator has three equal leg lengths, then it can be assembled such that it allows a self motion. It must be noted that for equal leg lengths some rigid assemblies also exist.

In the general case  $R_2 = R_3$ ,  $h_2 \neq 2$  we obtain again two conditions

$$M_1 : R_1 = 3h_2(h_2 - 2), \quad R_3 = 0, \quad M_2 : R_1 = 9, \quad R_3 = 3h_2^2 - 3. \quad (12)$$

$M_1$  yields no real solution and  $M_2$  yields a self motion, similar to the Case 1a, a spherical four bar-motion and rigid assemblies. As an example in Fig. 4 a 3-RPS manipulator is displayed, having the design parameters  $h_1 = 1, h_2 = 3$  and the leg lengths  $R_1 = 3, R_2 = R_3 = 2\sqrt{6}$ . On the left side two symmetric rigid assemblies are shown and **in a different view** on the right side a third assembly is added, where one can see that one leg is in the base plane. This assembly shows one pose of the one parameter self motion. In this **example** the transformation matrix reads

$$\mathbf{T}_1 = \begin{pmatrix} 1 & 0 & 0 & 0 \\ -4\sqrt{3}t & \frac{13}{3} - 8t^2 & -\frac{4\sqrt{2}\sqrt{3}}{3}A_1 B_1 & \frac{4\sqrt{3}}{3}A_1 t \\ -2\sqrt{3}B_1 t & \frac{4\sqrt{2}\sqrt{3}}{3}A_1 B_1 & \frac{13}{3} - 6t^2 & \frac{2\sqrt{3}}{3}B_1 t \\ 6t^2 - 5 & -\frac{4\sqrt{3}}{3}A_1 t & \frac{2\sqrt{3}}{3}B_1 t & 1 - 2t^2 \end{pmatrix}, \quad (13)$$

where  $A_1 = \sqrt{2 - 3t^2}$  and  $B_1 = \sqrt{9t^2 - 5}$ ,  $t \in \mathbb{R}$ .

**Case 2b:**  $R_2 \neq R_3$ . Like in the first case this yields the symmetric solutions.



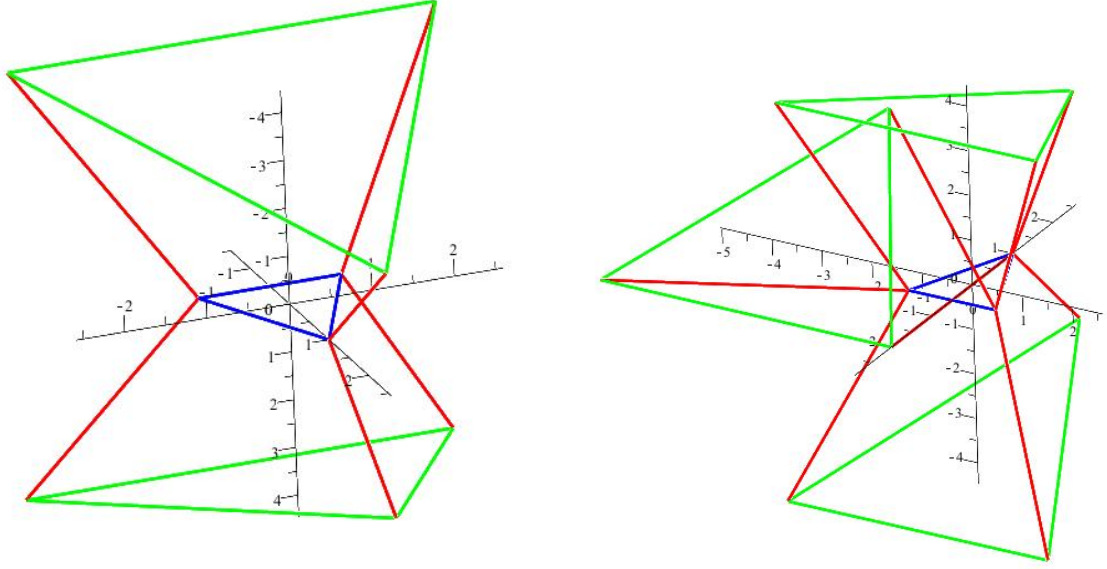


Figure 4: Case 2a:  $R_1 = 3, R_2 = R_3 = 2\sqrt{6}$

## 4 Transformation of the self-motions

The kinematic images of the self-motions described by the transformations in Eq. (8) and (13) are curves in  $\mathbb{P}^7$  which lie entirely on the Study-quadric. It would be possible to compute the transformation matrices even without specifying the design parameter  $h_2$ , but then the matrix becomes rather complicated and does not contain additional kinematic information. Therefore we stay with the example and set again  $h_2 = 3$ . Computing the Study-parameters of the transformation matrix  $\mathbf{T}_0$  yields

$$\gamma_0(t) = \kappa(\mathbf{T}_0) = (0 : 2\sqrt{2}A_0 : 6t : 2\sqrt{3}B_0 : -5\sqrt{3}B_0 : 3t : -\sqrt{2}A_0 : 0) \quad (14)$$

where  $A_0, B_0$  are defined as in Sec. 3 and  $t \in I \subset \mathbb{R}$ . The curve  $\gamma_0$  represents a self motion in the operation mode  $x_0 = 0$  of the 3-RPS manipulator. With a coordinate transformation  $\mathbf{T}_{B0}$  resp.  $\mathbf{T}_{M0}$  in the base and in the moving frame, the curve  $\gamma_0$  can be transformed **such that the curve passes through the kinematic image of the identity transformation**. After the transformation the curve is contained in the three dimensional generator space  $y_0 = y_1 = y_2 = y_3 = 0$  of the Study quadric, showing clearly that the motion is a spherical motion. Coordinate transformations in base and moving frame correspond to linear transformations in  $\mathbb{P}^7$  which map the Study-quadric to itself. The transformation matrices that change the coordinate systems in base and platform such that the motion passes through the identity read in this case

$$\mathbf{T}_{B0} = \begin{pmatrix} 2 & 0 & 0 & 0 & 0 & 0 & 0 & 0 \\ 0 & 2 & 0 & 0 & 0 & 0 & 0 & 0 \\ 0 & 0 & 2 & 0 & 0 & 0 & 0 & 0 \\ 0 & 0 & 0 & 2 & 0 & 0 & 0 & 0 \\ 0 & 0 & 0 & -2 & 2 & 0 & 0 & 0 \\ 0 & 0 & -2 & 0 & 0 & 2 & 0 & 0 \\ 0 & -2 & 0 & 0 & 0 & 0 & 2 & 0 \\ -2 & 0 & 0 & 0 & 0 & 0 & 0 & 2 \end{pmatrix}, \quad (15)$$



$$\mathbf{T}_{\mathbf{M}0} = \begin{pmatrix} 0 & 0 & -4 & -2\sqrt{2} & 0 & 0 & 0 & 0 \\ 0 & 0 & 2\sqrt{2} & -4 & 0 & 0 & 0 & 0 \\ 4 & -2\sqrt{2} & 0 & 0 & 0 & 0 & 0 & 0 \\ 2\sqrt{2} & 4 & 0 & 0 & 0 & 0 & 0 & 0 \\ 3\sqrt{2} & -6 & 0 & 0 & 0 & 0 & -4 & -2\sqrt{2} \\ 6 & 3\sqrt{2} & 0 & 0 & 0 & 0 & 2\sqrt{2} & -4 \\ 0 & 0 & 3\sqrt{2} & 6 & 4 & -2\sqrt{2} & 0 & 0 \\ 0 & 0 & -6 & 3\sqrt{2} & 2\sqrt{2} & 4 & 0 & 0 \end{pmatrix} \quad (16)$$

For a detailed description of the linear transformations in the kinematic image space and their corresponding matrices see [?, ?]. After applying the coordinate transformations to the curve  $\gamma_0$  its image  $\gamma'_0 = \mathbf{T}_{\mathbf{M}0} \cdot \mathbf{T}_{\mathbf{B}0} \cdot \gamma_0$  reads

$$\gamma'_0(t) = (-6t - \sqrt{2}\sqrt{3}B_0 : 3\sqrt{2}t - 2\sqrt{3}B_0 : -6A_0 : 2\sqrt{2}A_0 : 0 : 0 : 0 : 0), \quad (17)$$

where  $A_0$  and  $B_0$  are defined as above. In the representation of  $\gamma'_0$  (Eq.17) the last four Study-parameters vanish. This means that the motion generated by  $\gamma'_0$ , and therefore also the motion corresponding to  $\gamma_0$ , is a spherical motion (see Fig. 2 for  $h_2 = 3$  and in Fig. 3 for  $h_2 = 2$ ).

The self-motion in the operation mode  $x_1 = 0$  is represented by  $\mathbf{T}_1$  Eq.(13). The corresponding Study-parameters are

$$\gamma_1(t) = \kappa(\mathbf{T}_1) = (4\sqrt{3}A_1 : 0 : 6t : 2\sqrt{3}B_1 : -5\sqrt{3}B_1 : 3t : 0 : 10\sqrt{3}A_1) \quad (18)$$

where  $A_1, B_1$  and  $t$  are defined as above. Applying a coordinate transformation in the base resp. moving frame the curve  $\gamma_1$  is now transformed **such that the curve passes through the kinematic image of the identity transformation**. The transformation matrices  $\mathbf{T}_{\mathbf{B}1}$  and  $\mathbf{T}_{\mathbf{M}1}$  to perform this operation are identical to  $\mathbf{T}_{\mathbf{B}0}$  and  $\mathbf{T}_{\mathbf{M}0}$

$$\mathbf{T}_{\mathbf{B}1} = \mathbf{T}_{\mathbf{B}0}, \quad \mathbf{T}_{\mathbf{M}1} = \mathbf{T}_{\mathbf{M}0}.$$

After applying these transformations  $\mathbf{T}_{\mathbf{M}0} \cdot \mathbf{T}_{\mathbf{B}0} \cdot \gamma_1$  the image curve reads

$$\gamma'_1(t) = (-6t - \sqrt{2}\sqrt{3}B_1 : 3\sqrt{2}t - 2\sqrt{3}B_1 : 4\sqrt{3}A_1 : 2\sqrt{2}\sqrt{3}A_1 : 0 : 0 : 0 : 0). \quad (19)$$

This parametrization represents again a spherical motion. Note that this algorithm also works when the design parameter  $h_2$  is kept general in the equations. Then the motion representation is much more complicated, but one can see again that the last four Study parameters vanish. This proves that every self-motion of the 3-RPS parallel manipulator is a spherical motion. One can show that all the other possibilities of self-motions are symmetric cases of the cases discussed in this section.

## 5 Transition between the operation modes with self-motions

The 3-RPS parallel manipulator has two operation modes. In the previous sections it was shown that self-motions can appear in both operation modes when the manipulator is in a special pose having specific leg lengths  $r_i$ . The question arises if a transition between the operation modes can happen during a self-motion. It is clear that this can be possible only in very special poses. Such transition poses are represented by the points of intersection of the curves  $\gamma_0$  and  $\gamma_1$ , because in these poses a bifurcation is possible. These poses can be computed directly from the parametric representations of  $\gamma_0$  and  $\gamma_1$  in Eq. (14) and (18) without specifying the design parameter  $h_2$ . In the case of  $h_2 = 3$  the points of intersection of  $\gamma_0$  and  $\gamma_1$  correspond to the parameter values  $t_0 = t_1 = \sqrt{\frac{2}{3}}$ .

A general self-motion pose of the manipulator in the operation mode  $x_0 = 0$  is shown on the left side of Fig. 5. From this pose the manipulator can move during the self-motion into the “flat” pose shown in the middle of Fig. 5. To move out of this special pose there are two possible self-motion branches. The manipulator can stay in the same operation mode or it can branch into the other operation mode  $x_1 = 0$  as shown on the right side of Fig. 5.

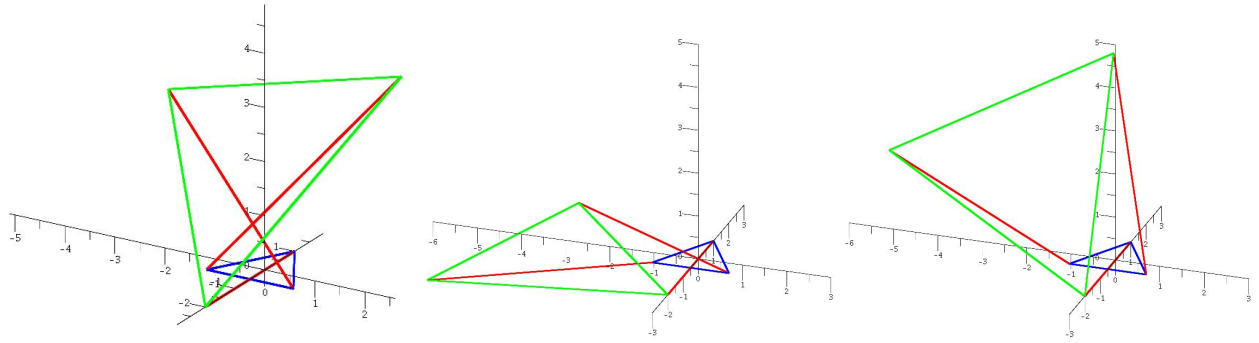


Figure 5: Changing the operation mode during a self-motion

## 6 Conclusion

Using the algebraic representation of constraint equations a complete classification of all self-motions of the 3-RPS parallel manipulator was given. A self-motion can appear only when the leg lengths have special values. There are self-motions in both operation modes of this manipulator. Using the kinematic images of the self-motions it was shown that all self-motions are spherical motions. They are either spherical four-bar motions or rotations, which were also formerly named butterfly motions. Remarkably it is also possible to change the operation mode in special branching poses of the self-motions.

## References